Available online at www.sciencedirect.com
ScienceDirect
Journal of Sound and Vibration 319 (2009) 807–821
JOURNAL OF SOUND AND VIBRATION
www.elsevier.com/locate/jsvi

On optimal design of half-wave resonators for acoustic damping in an enclosure

Ju Hyun Park, Chae Hoon Sohn*

Department of Mechanical Engineering, Sejong University, Seoul 143-747, Republic of Korea

Received 22 January 2008; received in revised form 23 June 2008; accepted 29 June 2008
Handling Editor: L.G. Tham
Available online 13 August 2008

Abstract

Acoustic design parameters of a half-wave resonator are studied experimentally for purely acoustic tuning of the resonator. According to the standard acoustic-test procedures, acoustic-pressure signals in the model enclosure with the resonators are measured. Based on the signals, quantitative acoustic properties of damping factor and sound absorption coefficient are evaluated and thereby, the acoustic-damping capacity of the resonator is characterized. Sound absorption coefficient has the advantages of the damping factor in various aspects. The coefficient indicates clearly the tuning frequency of the resonator, absorption effectiveness as a function of frequency, and overall damping capacity. The diameter and the number of a half-wave resonator, its distribution, and the blockage ratio at its inlet are selected as design parameters for optimal tuning of the resonator in the model enclosure. The resonators with larger diameter have the advantage of those with smaller one with respect to purely acoustic damping at the tuning frequency. The optimum number of resonators or the optimum open-area ratio decreases as boundary absorption decreases. When the open-area ratio exceeds the optimum value, over-damping appears, leading to a decrease in peak absorption coefficient and a broadening of absorption bandwidth. Blockage at the resonator inlet controls both peak absorption coefficient and its absorption bandwidth and it can be considered one of design factors for acoustic tuning.

1. Introduction

In liquid propellant rocket engines, injectors are mounted to the faceplate in order to inject propellants into the combustion chamber. Depending on the phase of the injected propellants, they are classified into liquid–liquid scheme and gas–liquid scheme injectors. In the pump-fed liquid rocket engines of high-performance, staged combustion cycle is usually employed, where preburner is used and regenerative cooling is adopted for the cooling of combustor wall [1]. In this system, the coaxial and gas–liquid scheme injector is typically used, which is illustrated in Fig. 1. As shown in this figure, gaseous oxidizer (GO_x) flows through the inner passage of the injector and then, it is mixed with liquid hydrocarbon fuel injected through several peripheral holes and finally, both GO_x and liquid fuel are injected into the chamber [2]. From the previous

*Corresponding author. Tel.: +82 2 3408 3788; fax: +82 2 3408 4333.
E-mail address: chsohn@sejong.ac.kr (C.H. Sohn).

0022-460X/$ - see front matter © 2008 Elsevier Ltd. All rights reserved.
doi:10.1016/j.jsv.2008.06.049

Nomenclature

B	blockage ratio at the resonator inlet, defined in Eq. (7)
c	sound speed in the medium
d_{in}	orifice diameter at the resonator inlet
d_{res}	inner diameter of the resonator
D_{en}	diameter of the model enclosure
f	frequency
f_0	tuning frequency or acoustic frequency of pressure oscillation in the model enclosure
H_{12}	transfer function defined in Eq. (2)
j	imaginary unit of complex number
k	wavenumber defined by $2\pi f/c$
l_{res}	length of the resonator
L_{en}	length of the model enclosure
p	acoustic-pressure amplitude measured by the microphone
P	signal transformed by fast Fourier transform (FFT)
r	normal incidence reflection factor
s	distance between the two microphones
x_1	distance between the resonator inlet and the further microphone (M1) location

Greek letters

α	sound absorption coefficient
α_I	integral or overall absorption coefficient defined in Eq. (6)
β	boundary absorption coefficient
Δl	length correction factor
η	damping factor defined in Eq. (1)
ρ	density
σ_A	open-area ratio, or the ratio of open area of the resonator to the mount-plane area

Subscripts

min	minimum value
max	maximum value
peak	peak response
res	resonator or state of the fluid in the resonator
0	state of the fluid in the model enclosure
1T	the first tangential acoustic mode
1L	the first longitudinal acoustic mode

work [3], it has been found first that the gas–liquid scheme injectors can play a significant role in acoustic damping like acoustic resonators in addition to its original function of propellants injection. It has been shown that the injector can absorb acoustic oscillation in the chamber most effectively when it has the tuning length of a half-wavelength with respect to the acoustic frequency to be damped. In other words, it has acted effectively as a half-wave resonator; the optimum length for acoustic tuning should be a half-wavelength in order to maximize acoustic absorption. In addition, high blockage at the injector inlet degraded acoustic damping with the optimum length adopted.

The previous study [3] suggested that a proper design of the injector can attenuate pressure oscillation to a good degree and eventually, we can do without additional installation of damping devices such as baffle and

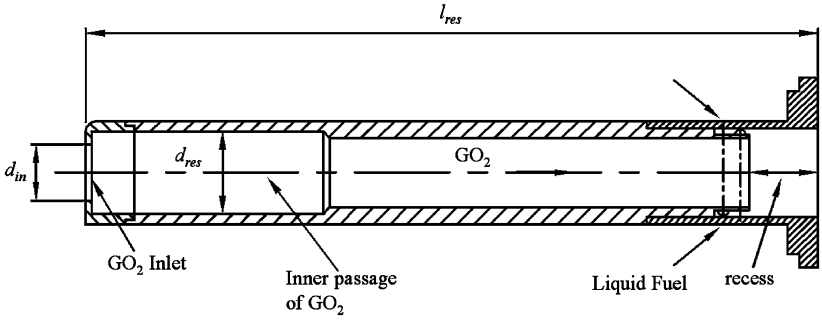

Fig. 1. Geometry of the coaxial and gas–liquid scheme injector, i.e., a half-wave resonator.

resonators for combustion stabilization [4]. In this regard, gas–liquid scheme injector can be considered as a half-wave resonator. The mechanism of acoustic damping or absorption occurring in a quarter-wave resonator [5–8] can be applied to a half-wave resonator as well. Accordingly, the tuning length of a half-wave resonator for maximum acoustic damping could be easily derived and verified [3]. But, there can be found only a little information on optimal tuning of quarter- or half-wave resonators. Several literatures [6,7,9] provide useful information on design procedures of typical resonators such as Helmholtz and a quarter-wave resonator, but not available design criterion on optimal tuning of a half-wave resonator. Accordingly, studies focused on acoustic function of a half-wave resonator are required for us to use it as an acoustic damper.

Since a half-wave resonator is an injector itself in a combustion chamber, a large number of the resonators are mounted and distributed uniformly on the faceplate. As aforementioned, a half-wave resonator functions solely as an acoustic resonator and it can be used for purely acoustic application. For this application, various design parameters of a half-wave resonator should be examined quantitatively from the standpoint of its optimal design and eventually, design criterion on the resonator should be made in available form. In this regard, in the present study, the diameter and the number of a half-wave resonator, its distribution, and the blockage at its inlet are selected as design parameters affecting the acoustic-damping capacity of the resonator in an enclosure in the present study. Acoustic damping can be investigated by various approaches [3,10–13]. In this study, effects of each parameter on acoustic damping are investigated experimentally by adopting linear acoustic test. Based on the experimental results, the present study provides practical design criteria or guidelines for optimal tuning of a half-wave resonator.

2. Experimental methods

2.1. Model enclosure and half-wave resonator

In the previous work [3], the acoustic field in a combustion chamber was calculated and it was shown that injectors or half-wave resonators damped out acoustic oscillations effectively in a chamber when it has the tuning length of a half-wave resonator. Here, instead of a combustion chamber, a model enclosure or an acoustic tube is adopted in order to quantify acoustic-damping properties of a half-wave resonator in the point of acoustic view.

The model enclosure has cylindrical shape with the inner diameter of 100 mm and the axial length of 300 mm. To damp out acoustic oscillations in the enclosure, single or numerous half-wave resonators are mounted to the circular side-plane of the enclosure. Although a half-wave resonator comes from gas–liquid scheme injector shown in Fig. 1, it is assumed to have complete cylindrical shape with two open ends and not to have recess for purely acoustic application. That is, the resonator is considered as a purely acoustic-damping device here, not an injector any more. Its optimal length, l_{res}, is already known from the previous study [3] and thus, it is fixed to be a half-wavelength, which is the optimum tuning length of the resonator. Here, the diameter of the resonator, d_{res}, and the inlet diameter, d_{in}, are adjusted for optimal tuning. Furthermore, the number of resonators and their distribution on the mount plane are also adjustable for its acoustic tuning. Both of the enclosure and the resonators are made of acrylic material. The medium in the enclosure is assumed to be a quiescent air of which density, ρ_0 and sound speed, c_0 are 1.2 kg/m^3 and 343 m/s, respectively.

2.2. Acoustic-test apparatus and experimental procedures

Several acoustic-damping properties or parameters can be adopted to evaluate acoustic-damping capacity of the resonator [6,14–16]. In our previous numerical study [3], the parameter of damping factor, η was selected out of them. In this study, sound absorption coefficient, α is adopted as another property because it is better quantitative parameter in various aspects. This point will be discussed in detail in later section.

Absorption coefficient can be measured by various standard methods such as impedance tube and reverberation room methods [14]. Here, transfer-function method is adopted, which is one of impedance tube methods. The details on the measurement method are described in the literature [17] and omitted here.

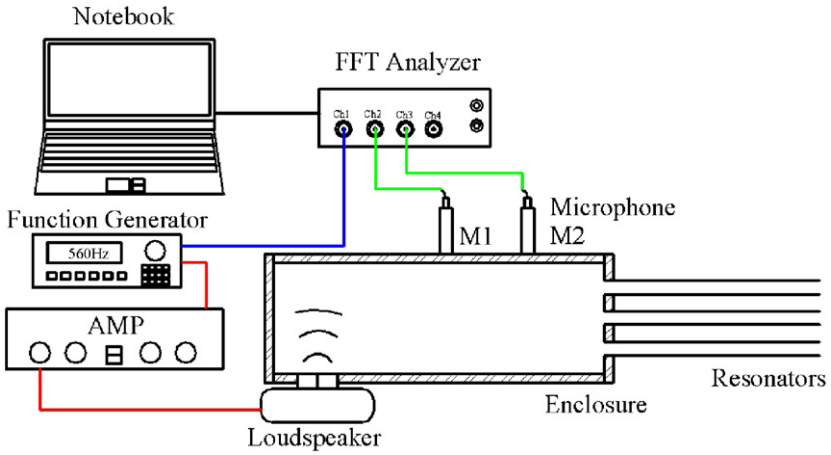

Fig. 2. Schematic diagram of acoustic-test apparatus ($D_{en} = 100$ mm and $L_{en} = 300$ mm).

According to the specifications of ISO-10534-2 [17], acoustic-test apparatus is set up and shown in Fig. 2. The enclosure, which corresponds to the impedance tube, is installed in the horizontal position at atmospheric pressure and 20 °C. For acoustic excitation, random-noise signal or monochromatic sinusoidal wave is generated by function generator, sent to amplifier (Inter M model QD-4960), where the signal is amplified, and finally sent to a loudspeaker. It is also sent to fast Fourier transform (FFT) spectrum analyzer through input-signal channel (Ch1) for synchronization with output or data signal-channels (Chs 2 and 3). The loudspeaker is located on the peripheral wall of the enclosure and imposes acoustic excitation into the enclosure. The present test is linear acoustic test, i.e., the amplitude of acoustic pressure excited in the enclosure is small and within a linear range. The enclosure made of acrylic material can easily vibrate, but our preliminary tests verified that the structural vibration of the enclosure did not affect the damping capability in a usual linear range of this acoustic excitation. The acoustic-pressure signals or responses from the enclosure are monitored by acoustic amplitude, which is measured by the microphones (M1 and M2). The microphone, M2 is installed 100 mm away from the resonator mount-plane of the enclosure and the distance between two microphones, M1 and M2 is 78 mm. Their locations correspond to the monitoring points. The signals measured by the microphones are sent to the spectrum analyzer, through which FFT is obtained. From FFT data, the acoustic resonance, the resonant frequencies, and the acoustic modes are identified. At the same time, quantitative acoustic properties of damping factor and absorption coefficient are also determined. The details on the acoustic test can be also found elsewhere [6,17]. Our preliminary tests verified that the present experimental apparatus offered reliable data of sound absorption coefficients with good accuracy.

In this work, the tuning length of a half-wave resonator, l_{res} may be selected arbitrarily and here, it is specified 300 mm. The length corresponds to the optimal length, i.e., a half-wavelength of the first longitudinal overtone mode travelling in the resonator with respect to the acoustic frequency of 572 Hz or so, which is close to f_{1T} observed in the specific chamber of the previous work [3]. That is, the resonator is tuned to acoustic oscillation of the frequency. But, considering mass or length correction factor, the tuning frequency of the resonator will be lowered more or less. It will be discussed later. Accordingly, acoustic oscillations with the frequencies of 300–800 Hz are excited by the loudspeaker and our preliminary experiment has verified that the random-noise signal has the constant acoustic intensity irrespective of frequency over the sweeping frequency range of 300–800 Hz.

The acoustic-pressure signals are measured in the enclosure mounted with half-wave resonator(s) as functions of the inner diameter of the resonator, the number of them, and its inlet diameter. Their distribution on the mount-plane of the enclosure is also considered. From the measured signals, acoustic-damping capacity of the resonator is evaluated by the acoustic properties of damping factor, η and absorption coefficient, α. The procedures to determine α are described in detail in Ref. [17] and omitted here. The larger η is and the closer α is to unity, the more effectively the resonator damps out acoustic oscillations.

3. Results and discussions

First, acoustic-damping capacity of the resonator is quantified by the acoustic properties. Next, effects of the resonator-design parameters on damping capacity are investigated. Based on them, design criteria or guidelines for the resonator are proposed to enhance acoustic-damping capacity. And finally, effects of blockage at the resonator inlet are examined.

3.1. Quantification of acoustic-damping capacity

In the enclosure with a single resonator of the variable inner diameter, d_{res} of 7–20 mm, acoustic-pressure responses are measured by M1 as a function of the excitation frequency and shown in Fig. 3. The signals measured by another microphone, M2 are similar to those shown in Fig. 3. From the acoustic amplitude in the enclosure without the resonator, it is found that this enclosure has a resonant peak of a longitudinal mode at $f_{1L} = 572$ Hz. Since acoustic damping is induced by installation of the half-wave resonator, the peak amplitude is decreased by the resonator. As shown in Fig. 3, peak amplitude becomes lower and the bandwidth is broadened as the inner diameter of the resonator is increased. This indicates that the resonator with larger diameter is more effective in acoustic damping or absorption. It is reasonable result, but in Fig. 3, there can be found one notable point not observed in the previous numerical work [3]. When the resonator is mounted, each resonant peak splits into two peaks and this mode split is more clarified with larger diameter. This phenomenon has been observed from time to time when Helmholtz or a quarter-wave resonator is installed [18] and it depends on the damping capacity of the resonator and the degree of wall-boundary absorption. It is known that the mode split occurs as acoustic damping increases and/or boundary absorption becomes small. The present enclosure and resonators are made of acrylic material on which the acoustic wave is dissipated only a little because its surface is smooth. That is, boundary absorption coefficient of the material will be small. In this situation, pure acoustic-cancellation effect of the resonator is more dominant over viscous dissipation or boundary absorption of acoustic energy on the material surface.

To evaluate acoustic-damping capacity of the resonator quantitatively, the parameter of damping factor, η may be adopted as in the previous work [3] and it is determined by bandwidth method in the form [3,6,19]

$$\eta = \frac{f_2 - f_1}{f_{peak}}, \tag{1}$$

where f_{peak} is the frequency at which the peak response (p_{peak}) appears and f_1 and f_2 are the frequencies at which the pressure amplitude corresponds to $p_{peak}/\sqrt{2}$ with $f_2 > f_1$. This equation indicates that the damping factor becomes higher as the bandwidth is broadened, i.e., acoustic resonance is weakened.

From the data shown in Fig. 3, the damping factor can be calculated by Eq. (1). But, mode split prevents us from finding the exact tuning frequency of the resonator and quantifying damping capacity clearly by the parameter, η. The tuning frequency of a resonator is the frequency to which the resonator is tuned. It should

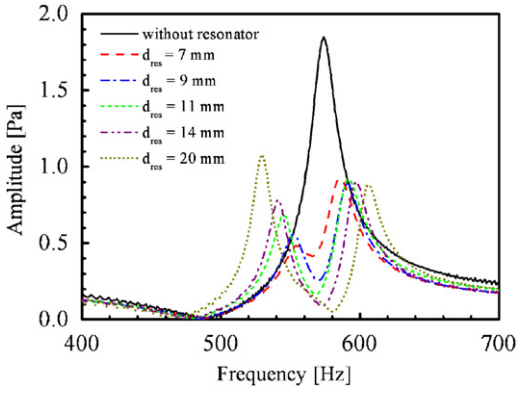

Fig. 3. Acoustic-pressure responses in the model enclosure without and with a single half-wave resonator for various diameters.

be as close to the frequency of harmful acoustic oscillation intended to be damped in the enclosure as possible. When one peak splits into two peaks by mode split, damping factor is not appropriate in evaluating acoustic-damping capacity of the resonator. Accordingly, the other quantitative parameter or property is required, which should represent damping capacity and avoid the ambiguity induced by the mode split. To meet these requirements, sound absorption coefficient, α [14,17] is adopted here. The higher damping capacity is, the larger the coefficient is. And its upper limit is 1.0, namely, 100%, which indicates that all the acoustic energy is absorbed by the acoustic-damping device. Accordingly, it has the physical meaning of absorption effectiveness.

The brief procedures to measure sound absorption coefficient are summarized as follows. First, the speed of sound, c in the enclosure is determined. While acoustic pressure is excited by the loudspeaker, acoustic amplitudes, p_1 and p_2 are measured as a function of time by two microphones, M1 and M2, respectively. The acoustic signals are transformed by FFT. From FFT data, the transfer function, H_{12} is obtained by the equation,

$$H_{12} = \frac{P_2}{P_1}, \tag{2}$$

where P_1 and P_2 denote the signals transformed from p_1 and p_2, respectively. The normal incidence reflection factor, r is calculated by the equation,

$$r = r_r + \mathrm{j}r_i = \frac{H_{12} - \mathrm{e}^{-\mathrm{j}ks}}{\mathrm{e}^{\mathrm{j}ks} - H_{12}} \mathrm{e}^{2\mathrm{j}kx_1}, \tag{3}$$

where r_r and r_i denote the real and the imaginary components of r, respectively, k is the wavenumber calculated by $k = 2\pi f/c$, s is the distance between the two microphones, and x_1 is the distance between the resonator inlet and the further microphone location. Then, sound absorption coefficient, α is finally calculated by the equation,

$$\alpha = 1 - |r|^2. \tag{4}$$

For a demonstration, absorption coefficients are determined as a function of the excitation frequency in the enclosure with a single resonator of $d_{\mathrm{res}} = 14\,\mathrm{mm}$ and shown in Fig. 4. Maximum value of α is observed at 558 Hz and it indicates that the present resonator is tuned to this frequency. And its value reaches 0.93. Compared with the damping factor, absorption coefficient quantifies acoustic-damping characteristics of the resonator more clearly.

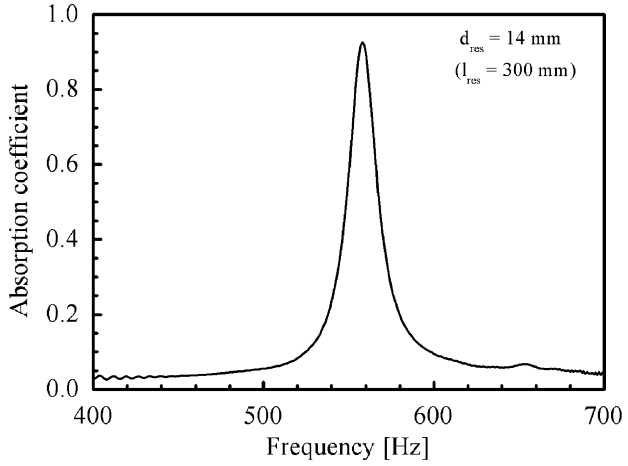

Fig. 4. Absorption coefficient of a single resonator as a function of frequency with $d_{\mathrm{res}} = 14\,\mathrm{mm}$ and $l_{\mathrm{res}} = 300\,\mathrm{mm}$.

3.2. Effects of design parameters on acoustic-damping capacity

The inner diameter of a half-wave resonator, the number of resonators, and their distribution on the mount plane of the enclosure are considered as the design parameters. Absorption coefficients are measured in the enclosure with the variable resonator diameter, d_{res} of 7–20 mm and shown in Fig. 5. As the resonator diameter increases, the peak or maximum value of α increases and the bandwidth of α is broadened. These can be predicted from the amplitude data shown in Fig. 3. On the other hand, the tuning frequency is lowered gradually with the diameter. This point can be explained as follows. The tuning frequency of a half-wave resonator is expressed by [3]

$$f_0 = \frac{c_{res}}{2(l_{res} + \Delta l)}, \tag{5}$$

where f_0 denotes tuning frequency, c_{res} sound speed of the fluid in the resonator, l_{res} the length of the resonator, and Δl length or mass correction factor. The length correction factor, Δl is proportional to d_{res} [6,7]. With l_{res} fixed, f_0 decreases with d_{res} as shown in Fig. 5, but its decrement is only within 2%. It is found that larger diameter of the resonator induces higher acoustic damping with respect to both peak absorption coefficient and the bandwidth. The resonator with $d_{res} = 20$ mm reaches $\alpha = 94\%$ or nearly 100% and the difference in α between $d_{res} = 14$ and 20 mm is only a little, which indicates that the diameter of 20 mm is close to the optimum diameter. Although not shown here, larger diameter than 20 mm showed rather smaller α, resulting from over-damping as reported in Ref. [6]. This result suggests that the optimum diameter of a half-wave resonator be between 14 and 20 mm. But, the optimum diameter will depend on not only the dimensional size of the enclosure but also the boundary absorption at wall. The dependence on the latter can be predicted from the results of the previous work [20] as well. The boundary absorption is fundamentally one of material properties of the solid body such as the resonator and the enclosure. As it decreases, the acoustic-damping effect of the resonator is enhanced at the tuning frequency [20]. Accordingly, with smaller boundary absorption, the optimum diameter of the resonator is lessened.

With the boundary absorption fixed, for a normalization of the diameter, we introduce an open-area ratio, σ_A, or the ratio of open area of the resonator to the mount-plane area. A single resonator with the diameter of 20 mm has $\sigma_A = 0.040$ in the present enclosure. It is predicted that the optimum value of σ_A is lower with smaller boundary absorption, which will be verified later.

To examine effects of the number of resonators, the resonators with $d_{res} = 7$ and 14 mm are selected. Their diameter ratio is exactly 1:2. The resonators with each diameter are distributed on the mount plane in the order demonstrated in Fig. 6. First, with the resonator of the smallest diameter, i.e., $d_{res} = 7$ mm, absorption coefficients measured for the variable number of resonators are shown in Fig. 7. In Fig. 7b, for a clearer demonstration, the peak values of α are plotted as a function of the number of resonators. And, integrals of α

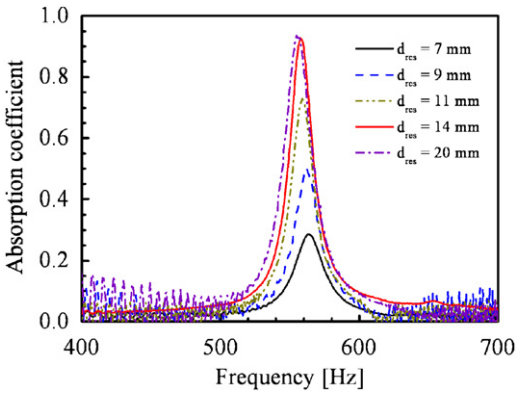

Fig. 5. Absorption coefficients of a single resonator as a function of frequency for several diameters.

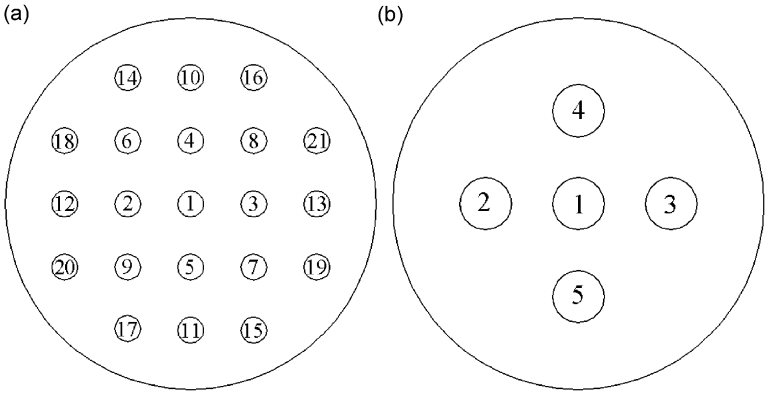

Fig. 6. Distributions of half-wave resonators with (a) $d_{res} = 7$ mm and (b) $d_{res} = 14$ mm (the number indicates the order of the resonator mounting).

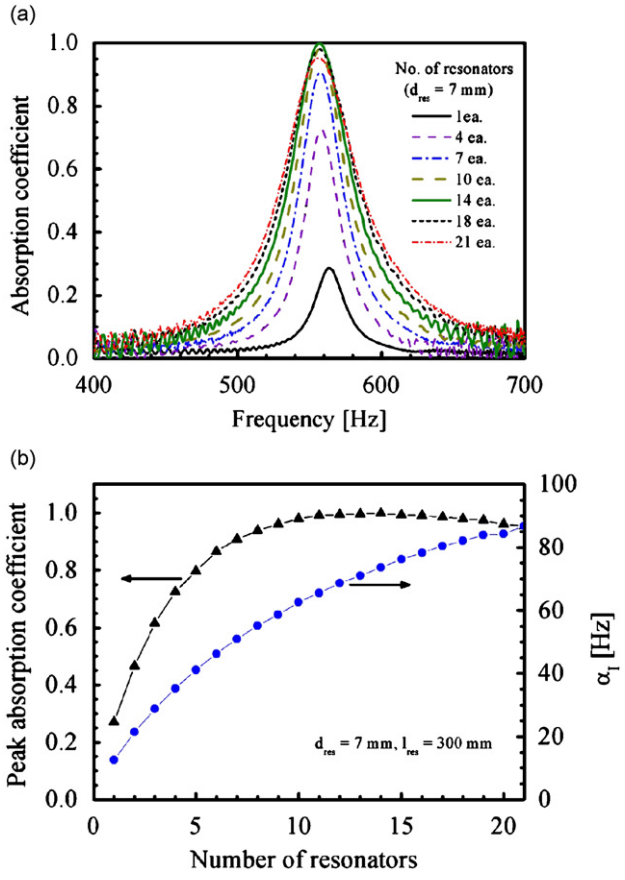

Fig. 7. Acoustic-damping capacity of the resonators with $d_{res} = 7$ mm for the various numbers of resonators: (a) absorption coefficients as a function of frequency and (b) peak absorption coefficient and integral absorption coefficient.

with respect to the frequency are also shown. The latter is introduced here to express overall damping capacity of the resonator and called overall or integral absorption coefficient, α_I. It is defined as

$$\alpha_I = \int_{f_{min}}^{f_{max}} \alpha \, df, \tag{6}$$

where f_{min} and f_{max} indicate minimum and maximum frequencies in the frequency range of interest, respectively. As shown in Fig. 7, the peak value of α increases with the number of resonators, and then, decreases after it reaches the highest value of 1.0 with 14 resonators. That is, the resonators with the number more than 14 show over-damping. The 14 resonators corresponds to $\sigma_A = 0.069$. On the other hand, both the bandwidth of α and the integral absorption coefficient, α_I increase continuously with the number.

There are expected two acoustic-damping mechanisms induced by installing half-wave resonators. One is acoustic-wave cancellation inside the resonator and the other is acoustic-energy dissipation by viscosity on the surface of the resonator. The former indicates pure or genuine acoustic-damping effect of the resonator. But, the former as well as the latter is affected by the boundary absorption at the surface as reported in Ref. [20]. The effect of the latter can be ensured from absorption coefficients in the non-tuning or mal-tuning frequency ranges in Fig. 7a. That is, in the frequency range far away from $f_0 = 564$ Hz, α increases continuously with the number of resonators in contrast to the tendency of the peak value of α. This is because the contact-surface area of the acoustic wave inside the resonators is proportional to the number of resonators.

Next, absorption coefficients of the resonators with $d_{res} = 14$ mm are measured for the various numbers of resonators and shown in Fig. 8. The two resonators have maximum α reaching 98% and then, decreases with the number of resonators. The two resonators' open-area ratio is $\sigma_A = 0.039$, which is the same as that of the eight resonators with $d_{res} = 7$ mm and of a single resonator with $d_{res} = 20$ mm as well. The dependences of peak α and absorption bandwidth on the number of resonators shown in Fig. 8 are the same as those shown in Fig. 7.

To obtain the same open-area ratio as that of 14 resonators with $d_{res} = 7$ mm, 3.5 resonators with $d_{res} = 14$ mm or 1.7 resonators with $d_{res} = 20$ mm are required. But, as shown in Fig. 8, the three resonators with $d_{res} = 14$ mm already cause over-damping. In case of $d_{res} = 20$ mm, there is no direct way to prove whether a single resonator shows over-damping or not. But, from the results shown in Figs. 5 and 8, it is predicted that a single resonator with $d_{res} = 20$ mm shows over-damping or optimum damping. This indicates that the smaller number of resonators is required for optimum damping as the resonator diameter increases. That is, the optimum open-area ratio decreases with the resonator diameter. This correlation between the optimum open-area ratio and the resonator diameter can be explained as follows. The aforementioned boundary absorption fundamentally depends on the material property. But, it is affected physically by the circumferential surface area of the resonator. Accordingly, when the same material is adopted, the more resonators with smaller diameter give higher boundary absorption with the open-area ratio fixed. The higher boundary absorption degrades pure or genuine acoustic-damping effect induced by the resonator at the tuning frequency. For this reason, the resonators with larger diameter have the advantage of those with smaller one for higher peak absorption at f_0.

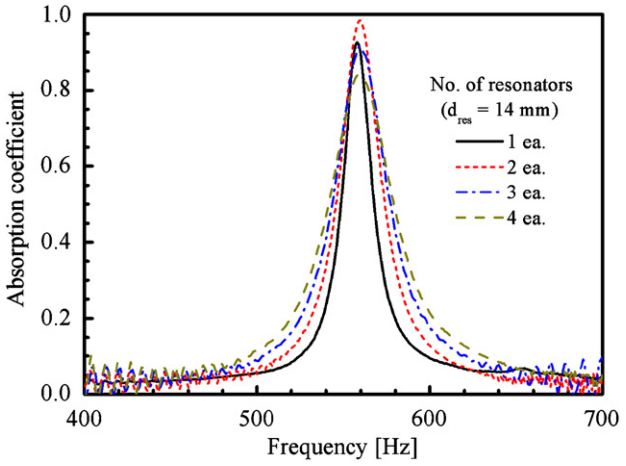

Fig. 8. Absorption coefficients of the resonators with $d_{res} = 14$ mm for the various numbers of resonators.

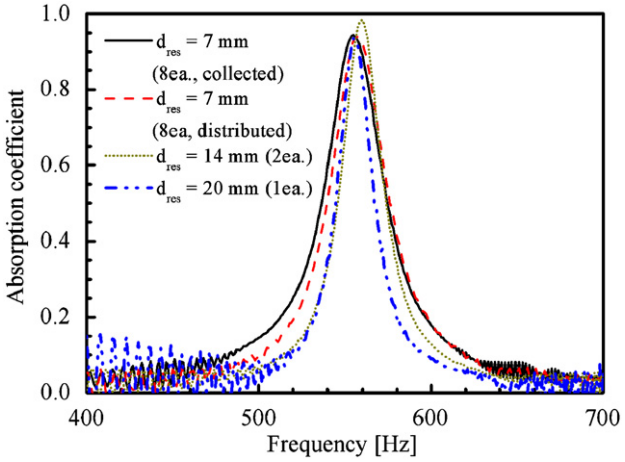

Fig. 9. Absorption coefficients of the resonators for various diameters with the identical open-area ratio.

All of three cases, i.e., the eight resonators with $d_{res} = 7$ mm, the two resonators with $d_{res} = 14$ mm, and a single resonator with $d_{res} = 20$ mm have the nearly identical open area. The absorption coefficients of them are shown as a function of frequency in Fig. 9. The two resonators with $d_{res} = 14$ mm have better acoustic-damping capacity than the eight resonators with $d_{res} = 7$ mm. This is because the former has smaller surface area than the latter as aforementioned. But, a single resonator with $d_{res} = 20$ mm has worse damping capacity than the two resonators with $d_{res} = 14$ mm and similar capacity to that of the eight resonators with $d_{res} = 7$ mm. This point verifies that over-damping appears in case of a single resonator with $d_{res} = 20$ mm.

In Fig. 9, the effect of the resonators' distribution on the mount plane of the enclosure can be also examined. The eight compactly collected resonators with $d_{res} = 7$ mm are compared with the identical number of resonators distributed uniformly on the mount plane. As shown in the figure, the difference in absorption coefficient between two cases is negligibly small. Accordingly, the resonators' distribution is not a critical design factor of a half-wave resonator.

To support directly the dependence of the optimum open-area ratio or the optimum number of resonators on boundary absorption, supplementary numerical analysis is conducted with boundary absorption coefficient, β [3] adopted. It is the acoustic analysis proposed in Refs. [3,10], where details on numerical methods and procedures can be found. From numerical calculation, the optimum number of the resonator is found as a function of β, which is treated as a material property of the resonator and the enclosure. Because it is difficult to find the materials with a wide range of β, numerical analysis has been adopted instead of experimental investigation. The optimum number of resonators, which produces the peak α equal to unity, is shown as a function of β in Fig. 10. For example, with $\beta = 7.57 \times 10^{-4}$, the optimum number is 14. The optimum number depends on β and the optimum number decreases as β decreases. With the open-area fixed, an increase in the diameter of resonator corresponds to a decrease in β. The results shown in Fig. 10 support the correlation between the optimum open-area ratio and the resonator diameter aforementioned.

By changing the shape of the cross-section of the resonator, boundary absorption can be also adjusted. For example, circular, rectangular, and triangular cross-sections are selected for comparison of their absorption capacity. With the identical cross-sectional area, the ratio of three peripheral or circumferential lengths is about 1.00:1.13:1.29. That is, the circular shape has the smallest surface area and triangular one has the largest. From numerical analysis, it is found that the circular shape comes the first, rectangular the next, and triangular the last in descending order of the peak absorption coefficient, which is reasonable result. For example, with $\beta = 0.001$ and a single resonator of the circular shape of $d_{res} = 14$ mm, its sound absorption coefficient is calculated to be 0.86. Rectangular and triangular ones are 0.83 and 0.79, respectively. When they are normalized by the absorption coefficient of the circular one, they are 1.00, 0.97, and 0.92, respectively.

In conclusion, with a half-wave resonator, design criterion for 100% acoustic absorption at the tuning frequency cannot be suggested in the form of '$\sigma_A =$ constant' because even purely acoustic-damping effect

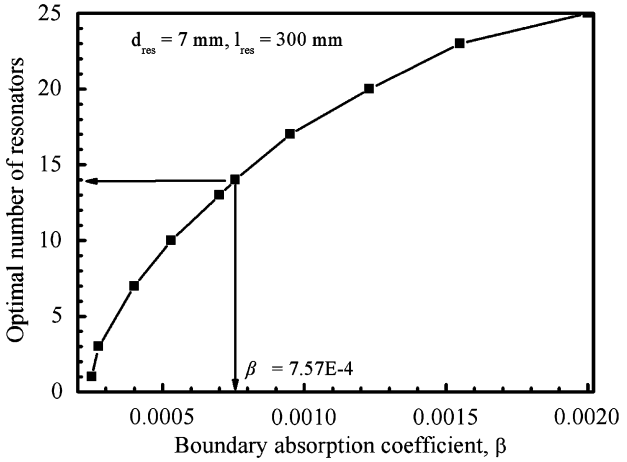

Fig. 10. Optimal number of the resonators with $d_{res} = 7$ mm as a function of boundary absorption coefficient.

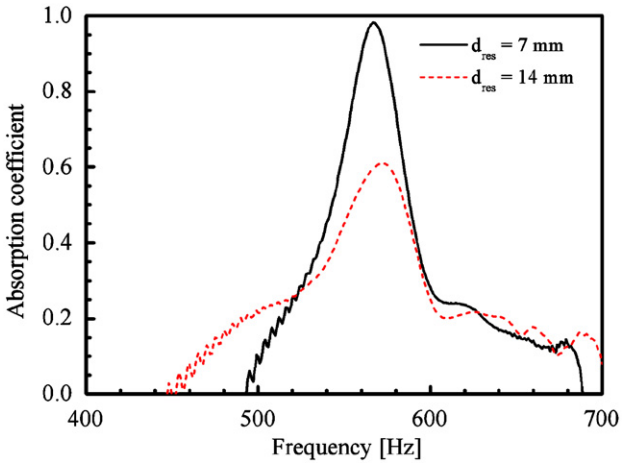

Fig. 11. Absorption coefficients of two single resonators with $d_{res} = 7$ and 14 mm, respectively, as a function of frequency ($D_{en} = 35$ mm).

depends on the geometry as well as the material property. On the other hand, for broad sound absorption in a wider frequency range near the tuning frequency, the resonators with higher boundary absorption are more effective. That is, the large number of resonators and the reduction of its diameter are desirable for this purpose.

When the open-area ratio exceeds the optimum value, the peak absorption coefficient begins to decrease, leading to over-damping as shown in Fig. 7a. As another way to increase the open-area ratio, the diameter of the enclosure is reduced to from 100 to 35 mm. Two single resonators with $d_{res} = 7$ and 20 mm, respectively, are installed in the enclosure with the reduced diameter of 35 mm. The measured absorption coefficients in two cases are shown in Fig. 11. In contrast to the results shown in Fig. 5, the resonator with larger diameter has lower absorption capacity, which results from over-damping. In this case, the optimum diameter is about 7 mm.

3.3. *Effects of inlet blockage on acoustic absorption*

In the preceding section, with the resonator length fixed, effects of design parameters of a half-wave resonator on acoustic absorption or damping are discussed. Inlet blockage can be also one of design

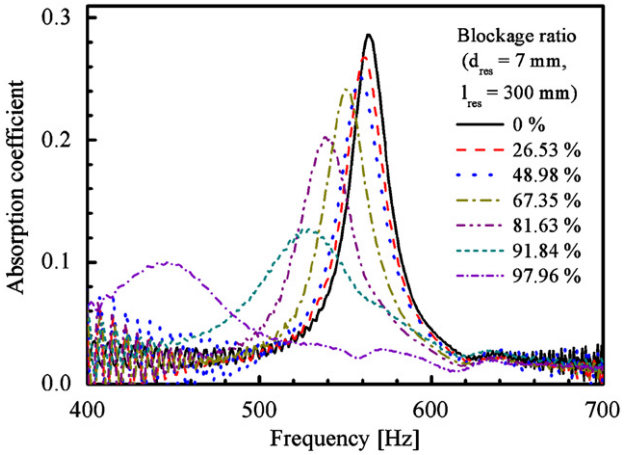

Fig. 12. Absorption coefficients of the resonators with the optimum length as a function of frequency for various blockage ratios.

parameters, but its acoustic effect is discussed separately in this section because design of blockage is closely coupled with the resonator length as reported in the previous work [20].

In the previous work [20], the damping factor, η was calculated as a function of blockage ratio in two cases of optimum and non-optimum length resonators. And, it was reported that each resonator with a specific length has its optimum blockage ratio. In the present study, absorption coefficients are measured instead of damping factor and with the aid of the acoustic property of α, new findings on acoustic tuning of a half-wave resonator are found. First, a single injector of the optimum length ($l_{res} = 300$ mm) with $d_{res} = 7$ mm is installed and its absorption coefficient is shown as a function of frequency for various blockage ratios in Fig. 12. Blockage ratio, B is defined as [3],

$$B = \frac{d_{res}^2 - d_{in}^2}{d_{res}^2}, \tag{7}$$

which denotes the ratio of the blocked area to the resonator cross-sectional area at the resonator inlet. The resonator with $d_{res} = 7$ mm is tuned to the tuning frequency of 564 Hz as shown in Fig. 5, which is confirmed by $f_0 = 564$ Hz at $B = 0\%$ in Fig. 12. As B increases, two phenomena are observed. One is a decrease in peak α and the other is a broadening of absorption bandwidth. The former can be explained by the change of boundary condition at the resonator inlet. That is, when some part of the resonator inlet is blocked, acoustically open boundary condition of acoustic impedance, $Z = 0$ is not maintained at the blocked part. And then, the wavelength of the acoustic wave oscillating inside the resonator is elongated to meet the modified boundary condition. This causes the tuning frequency to decrease with the blockage ratio on the average although the wavelength is maintained at the open part near the centerline. The latter phenomenon, i.e., a broadening of bandwidth results from the same reason. By partial blockage at the resonator inlet, the waves with wider range of wavelengths travels inside the resonator, leading to a broadening of α curve near the tuning frequency. It is also noteworthy that the integral absorption coefficient, α_I, defined by Eq. (6), maintains nearly constant value (≈ 15 Hz) irrespective of the blockage ratio. This indicates that damping capacity of the resonator does not depend on the blockage ratio with respect to integral or overall damping. According to the design requirement, suitable combination of the value of peak α and the absorption bandwidth will be accomplished by the adjustment of blockage ratio.

Next, absorption coefficients of a single resonator of a non-optimum length ($l_{res} = 280$ mm) with $d_{res} = 7$ mm are measured and shown in Fig. 13. From the figure, it can be easily found that the tuning frequency shifts from 564 to 606 Hz at $B = 0\%$. In this regard, absorption-coefficient approach is more useful because the modified tuning frequency could not be found by damping-factor approach [3,20] with the enclosure or chamber unchanged. As observed in Fig. 13, peak α decreases and absorption bandwidth is

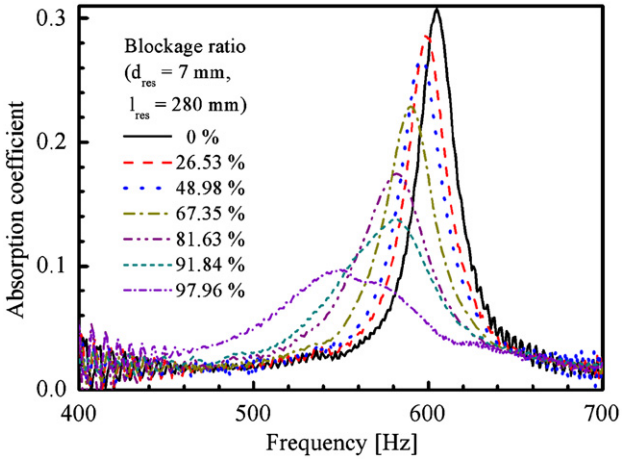

Fig. 13. Absorption coefficients of the resonators with a non-optimum length as a function of frequency for various blockage ratios.

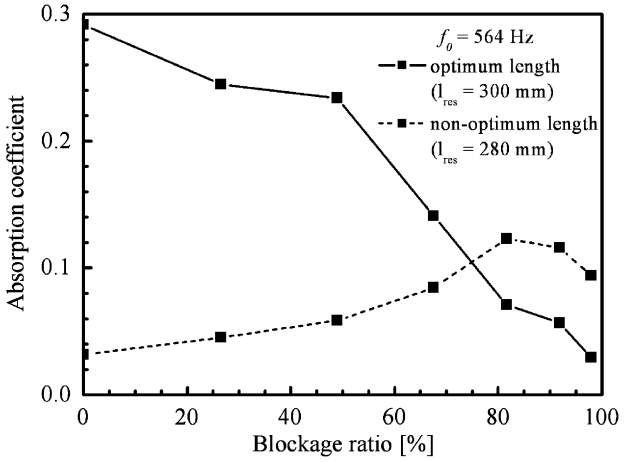

Fig. 14. Absorption coefficients of the resonators with optimum and non-optimum lengths at the tuning frequency of 564 Hz.

broadened as B increases. From Figs. 12 and 13, absorption coefficients at $f_0 = 564$ Hz, which is the tuning frequency of the optimum-length resonator, are extracted and shown as a function of B in Fig. 14. As predicted, in case of the optimum-length injector, absorption coefficient decreases continuously with the blockage ratio. On the other hand, in case of the non-optimum length, it increases gradually with blockage ratio, reaches its maximum value at a specific blockage ratio, and then, decreases with B. It supports that the optimum blockage ratio varies with the resonator length.

4. Conclusion

Various design parameters of a half-wave resonator have been examined experimentally from the standpoint of its optimal design for purely acoustic applications. According to the standard acoustic-test procedures, experiments have been conducted and acoustic-pressure signals in a model enclosure have been measured. Based on the signals, quantitative acoustic properties have been calculated, which are used to characterize acoustic-damping capacity of the resonator as an acoustic damper.

As a quantitative property of the resonator, sound absorption coefficient, which has the physical meaning of sound absorption effectiveness, shows more advantages over the damping factor in various aspects.

The coefficient indicates clearly the tuning frequency of the resonator, absorption effectiveness as a function of frequency, and overall damping capacity. Furthermore, it indicates both peak absorption value and the bandwidth of absorption at the same time. When blockage at the resonator inlet is made, the optimum tuning length of the resonator can be found easily as a function of the blockage ratio judging from absorption coefficient.

To provide design criteria or guidelines for optimum tuning of a half-wave resonator, the diameter and the number of a half-wave resonator, the resonators' distribution, and the blockage at its inlet have been selected as design parameters affecting the acoustic-damping capacity of the resonator in a model enclosure. The resonators with larger diameter have the advantage of those with smaller one with respect to pure acoustic damping at the tuning frequency. This is because the more resonators with smaller diameter have higher boundary absorption with the open-area ratio fixed when the same material is adopted. The optimum number of the resonators or the optimum open-area ratio depends on boundary absorption. It decreases as boundary absorption decreases. It is worth noting that boundary absorption depends on geometric parameters as well as material property of the resonator. Accordingly, the enlargement of the resonator diameter is desirable. When the open-area ratio exceeds the optimum value, over-damping appears, resulting in a decrease in peak absorption coefficient and a broadening of absorption bandwidth at the same time. On the other hand, for broad sound absorption in the wider frequency range near the tuning frequency, the resonators with rather higher boundary absorption are more effective. That is, the large number of the resonators and a reduction of the resonator diameter are desirable methods for this purpose. With respect to the resonators' distribution on the mount plane, the experimental results showed that the distribution of the resonators is not a critical design factor.

When blockage at the resonator inlet is applied, several acoustic effects can be produced. It has been found that blockage controls both the value of peak absorption coefficient and the absorption bandwidth. And, the present results showed that the optimum tuning length of the resonator depends on the blockage ratio and it decreases with the ratio. Accordingly, blockage can be considered one of design parameters affecting acoustic properties of the resonator although blockage has not been an original design parameter of the acoustic resonators. The parameter of inlet blockage will help to enhance the flexibility in designing the resonators. Although design criteria or guidelines for optimum design of a half-wave resonator are concentrated on in this study, the present findings are not limited to the specific resonator, but applicable to the other resonators with the same damping mechanism as a half-wave resonator.

References

[1] D.K. Huzel, D.H. Huang, *Modern Engineering for Design of Liquid-Propellant Rocket*, *Progress in Astronautics and Aeronautics*, Vol. 147. AIAA, Washington, DC, 1992, p. 35.

[2] G.P. Sutton, History of liquid-propellant rocket engines in Russia, formerly the Soviet Union, *Journal of Propulsion and Power* 19 (2003) 1008–1037.

[3] C.H. Sohn, I.-S. Park, S.-K. Kim, H.J. Kim, Acoustic tuning of gas–liquid scheme injectors for acoustic damping in a combustion chamber of a liquid rocket engine, *Journal of Sound and Vibration* 304 (2007) 793–810.

[4] K.R. McManus, T. Poinsot, S.M. Candel, A review of active control of combustion instabilities, *Progress in Energy and Combustion Science* 19 (1993) 1–29.

[5] D.J. Harrje, F.H. Reardon, *Liquid Propellant Rocket Combustion Instability, SP-194*, NASA, 1972.

[6] E. Laudien, R. Pongratz, R. Pierro, D. Preclik, Experimental procedures aiding the design of acoustic cavities, in: V. Yang, W.E. Anderson (Eds.), *Liquid Rocket Engine Combustion Instability*, *Progress in Astronautics and Aeronautics*, Vol. 169, AIAA, Washington, DC, 1995, pp. 377–399.

[7] R.B. Keller Jr., *Liquid Rocket Engine Combustion Stabilization Devices, SP-8113*, NASA, 1974.

[8] R. Glav, P.-L. Regaud, M. Abom, Study of a folded resonator including the effects of higher order modes, *Journal of Sound and Vibration* 273 (2004) 777–792.

[9] P.K. Tang, W.A. Sirignano, Theory of a generalized Helmholtz resonator, *Journal of Sound and Vibration* 26 (1973) 247–262.

[10] T. Tsuji, T. Tsuchiya, Y. Kagawa, Finite element and boundary element modelling for the acoustic wave transmission in mean flow medium, *Journal of Sound and Vibration* 255 (2002) 849–866.

[11] D. Li, L. Cheng, Acoustically coupled model of an enclosure and a Helmholtz resonator array, *Journal of Sound and Vibration* 305 (2007) 272–288.

[12] P.K. Tang, D.T. Harrje, W.A. Sirignano, Experimental verification of the energy dissipation mechanism in acoustic dampers, *Journal of Sound and Vibration* 26 (1973) 263–267.

[13] Y.Y. Lee, E.W.M. Lee, C.F. Ng, Sound absorption of a finite flexible micro-perforated panel backed by an air cavity, *Journal of Sound and Vibration* 287 (2005) 227–243.
[14] F. Fahy, *Foundations of Engineering Acoustics*, Elsevier, UK, 2001 (Chapter 7).
[15] P.M. Morse, K.U. Ingard, *Theoretical Acoustics*, McGraw-Hill, Inc., USA, 1968 (Chapter 9).
[16] L.E. Kinsler, A.R. Frey, A.B. Coppens, J.V. Sanders, *Fundamentals of Acoustics*, fourth ed., Wiley, New York, 2000 (Chapter 2).
[17] ISO 10534-2, Acoustics—determination of sound absorption coefficient and impedance in impedance tubes—part 2: transfer-function method, 1998.
[18] M.S. Natanzon, *Combustion Instability*, Mashinostroyeniye, Moscow, Russia, 1986 (Chapter 3).
[19] S.-K. Kim, H.J. Kim, W.S. Seol, C.H. Sohn, Acoustic stability analysis of liquid propellant rocket combustion chambers, AIAA Paper 2004-4142, July 2004.
[20] C.H. Sohn, I.-S. Park, Effects of inlet blockage of gas–liquid scheme injector on acoustic tuning for acoustic damping in a combustion chamber, *Journal of Mechanical Science and Technology* 22 (2008) 330–337.